

CHEMISTRY OF MACRO CYCLES CONTAINING ONLY SULFUR DONORS; SOME NOTEWORTHY RESULTS

Abstract

Thiamacrocyclics how rich Coordination chemistry, producing isolated as well as polymeric metallo-supra molecular frameworks. Thia-donor networks' attraction towards soft metal ions and their capacity to help stabilising uncommon oxidation states for some metals are what define the way they interact. It is seen that thioether sulphur employed in a flexible macrocyclic framework will adopt a combination of an *endo*- and an *exo*- positioning with regard to that macrocyclic cavity, providing the development of endocyclic as well as exocyclic metal complexes. Additionally, the existence of *exo*-oriented Sulfer-donors being desirable synthetically because it offers a way to create S-bridged frameworks, which frequently correlate with lesser prevalent (and occasionally novel) compounds like a variety of polymeric metal coordination networks. The adoption of these strategies has frequently led to an array of unique and uncommon metallo-structures, as described in this article.

Authors

Partha Pratim Das

P. G. Department of Chemistry
Magadh University,
Bodh-Gaya, Bihar, India.

I. INTRODUCTION

Since the groundbreaking discoveries of Pedersen¹, Lehn², and Cram³, which involved the production of cation specific crown ethers, cryptands, and spherands, the design and manufacturing of macrocycles with very specific sensors for metal's cations is continuing to advance. The potential of macrocyclic ligands as selective metal-ion binding agents has been extensively studied. The cyclic structure of macrocycles, that includes an inbuilt receptor cavity as the metal bonding site, renders them suitable for this function. The macrocyclic ring's constrained conformational flexibility helps to fit the metal ion's steric (and electrical) needs according to the macrocycle's cavity dimensions. There are several uses for macrocycles, particularly in the sensing as well as separating of diverse materials⁴. The macrocycle effect⁵, which occurs when macrocyclic ligand compounds outperform their open-chain counterparts in terms of kinetic as well as thermodynamic stability, led to their adoption as reliable building blocks⁶ for the construction of supramolecular structures. The metal ion in the aforementioned situations often exhibits *endo*-(in cavity) [Figure 1A] binding. There are currently a lot of instances of macrocyclic frameworks that show metal ion bonding *exo*- [Figure 1B] to their macrocyclic cavities, albeit being less prevalent. A lesser number of *endo*-/*exo*- structures, including homo- and heteronuclear *endo*-/*exo*- frameworks, have been constructed using ring structures that concurrently exhibit both *endo*- and exocyclic coordination to produce final structures that specifically represent the existence of dual coordination types [Figure 1C and 1D]. *Exo*-coordination is frequently, but not exclusively, connected with macrocycles that include thioether⁷. Numerous researches are being done on macrocycles with O, S, Se, and Te, as donating atoms. O, S- containing macrocycles are most common. Over the years, macrocycles with both mixed hard and soft donor atoms have found significance because they have the ability to bind two metals with different properties and oxidation states together in a single cavity. In this chapter, chemistry of macrocyclic ligands incorporating mainly all sulfur donor atoms is discussed categorically.

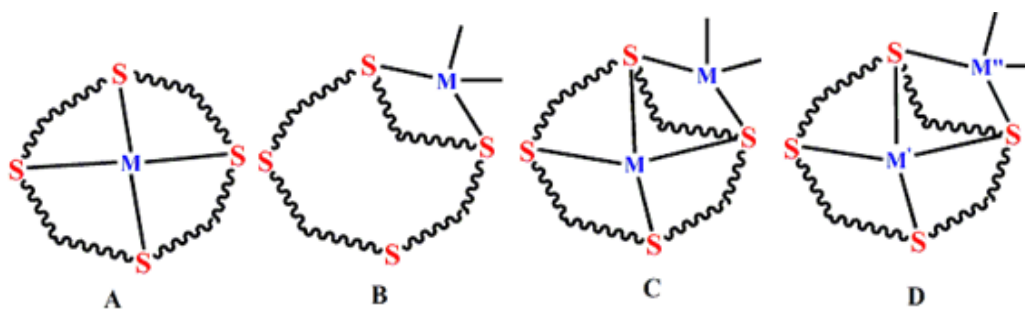


Figure 1

II. ALL SULFUR MACROCYCLES AND THEIR METAL COMPLEXES

With 1,4,7 trithiacyclononane (L^1) and 1,4,7,10-tetrathiacyclododecane (L^4)⁸; $[Cd(L)_2]X_2$ type of bi-ligand Cd^{II} complexes have been synthesized. Both L^1 ligands interact facially in $[Cd(L^1)_2](PF_6)_2$ [Figure 3a] to form an architectural configuration with distorted octahedral coordination shape. In $[Cd(L^4)_2](ClO_4)_2$ [Figure 3b], each L^4 connects to its four sulfur atoms, resulting in a unique S_8 distorted square anti-prismatic coordination structure that resembles a sandwich. Numerous such ligands are reported in

literature. Few of them are shown in Figure 2. Similar such compounds were reported, Such as, $[\text{Hg}(\text{L}^6)](\text{ClO}_4)_2$, $[\text{Cd}(\text{L}^6)](\text{ClO}_4)_2$, $[\text{Hg}(\text{L}^6)\text{Cl}_2]$ etc.

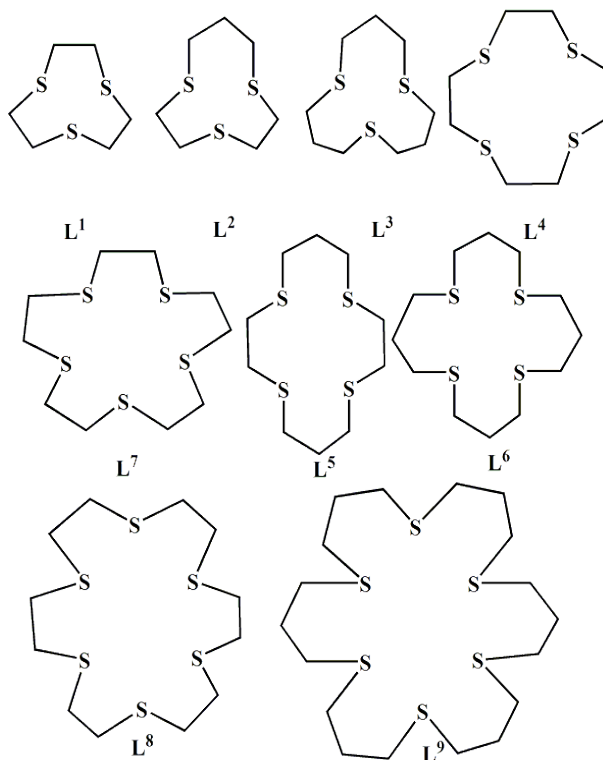
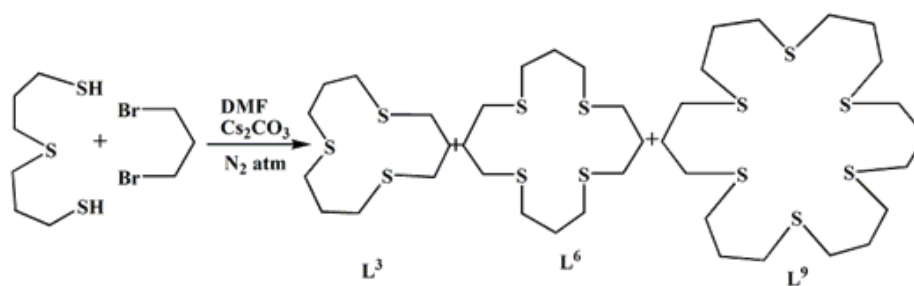


Figure 2

L^1 produces square planar compound, $\text{cis}[\text{Pd}(\text{L}^1)\text{Cl}_2]$ ⁹[Figure 4a], indicating the propensity of Pd^{II} to generate square-planar compound with a combination of neutral ligand and halides. Just two among three available S donors of L^1 are bonded, as can be seen in the structure. The last S atom nevertheless is placed at the axial Pd-S distant connection proximity of 3.16 \AA over the PdS_2Cl_2 coordination plane. Additionally, the Pd^{II} core is 3.53 \AA away from one thioether donor of a nearby compound.

Such Ligands are synthesized by a generalized procure of reaction between appropriate thiol precursor and dibromo alkane in DMF under nitrogen atmosphere. Generally mixture of ligands are produced which are then purified by chromatographic separation. One such scheme of reaction in shown in Scheme 1, below¹⁰:



Scheme 1

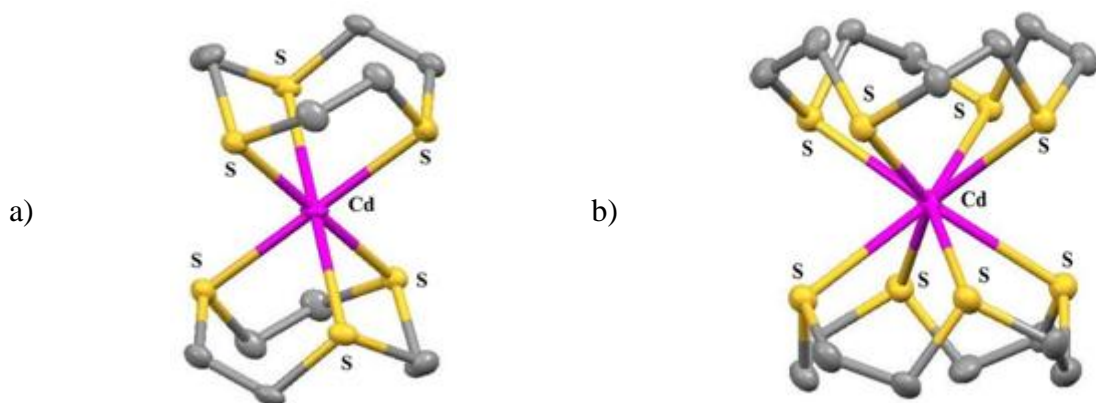


Figure 3

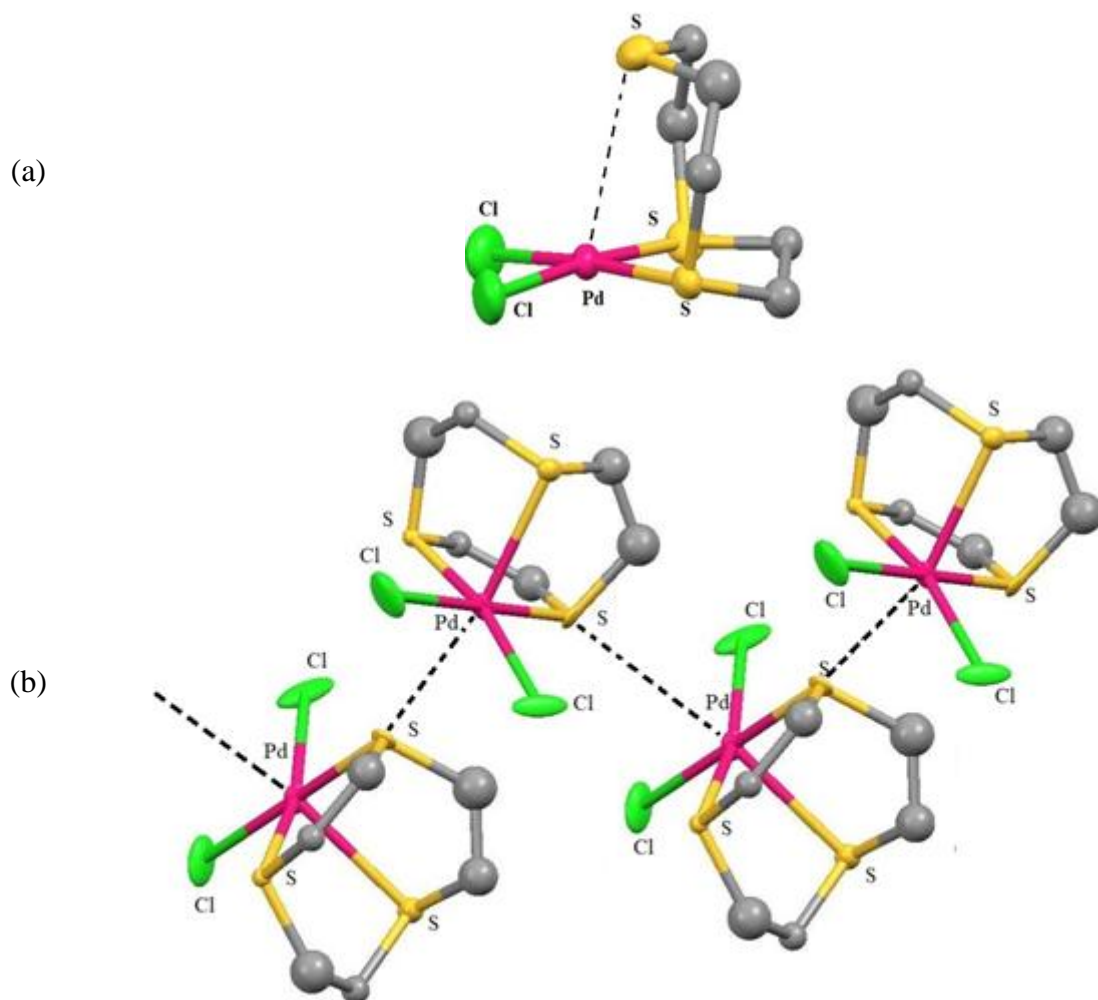


Figure 4

An X-Ray analysis of the structural framework of *cis*-[Pd(L¹)Cl₂] at different pressures revealed that, at 4.4 GPa, an abrupt shift from the mononuclear square planar framework to a zigzag chain polymer [Figure 4b] took place, along with a significant conformational modification to a portion of the bound macrocycle's backbone. Each Pd^{II}

center has a pseudo-octahedral architecture as a result of the contraction of the in-plane Pd-S and above-plane Pd-S lengths to 2.85 and 3.12 Å, respectively. The transition is reversible when the pressure is reduced.

In the framework of $[\text{Pt}(\text{L}^1)(\text{tmphen})](\text{PF}_6)$ [Figure 5], the compound assumes a *cis*-square-planar setup, with the bidentate tmphen ligand occupying two slots of the square and the thioether donors from L^1 filling the other two. These Pt-S bond lengths at 2.27 and 2.26 Å, respectively, are not exceptional. A lengthy connection of 2.88 Å, develops to the Platinum (II) core due to the third macrocyclic thioether atom's intriguing placement above the square plane, giving the Pt center a pseudo-5-coordination, distorted square pyramidal shape generally.

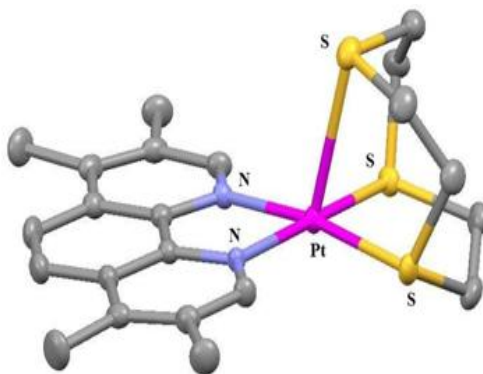
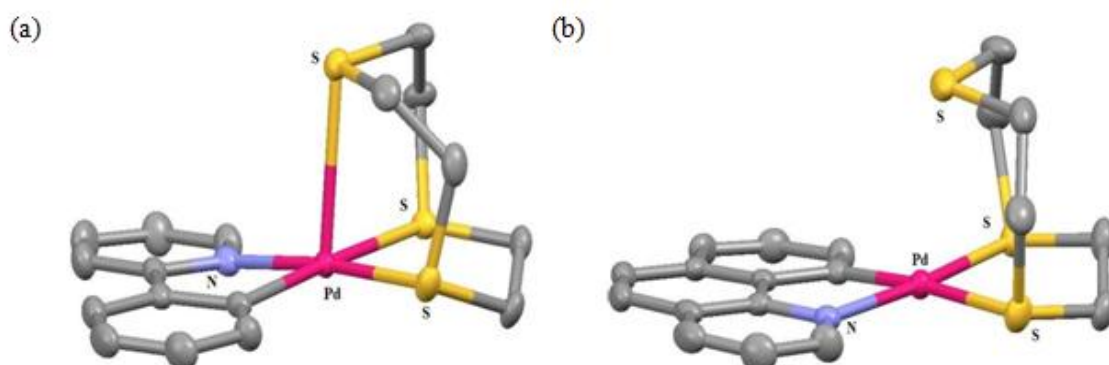


Figure 5

Numerous mixed-ligand Pd^{II} and Pt^{II} compounds of the type $[\text{ML}(\text{L}^1)](\text{PF}_6)$, where M is either palladium(II) or platinum(II); L is either ppy (2-phenyl pyridine) [Figure 6a], bzq (7,8-benzoquinolate) [Figure 6b, 6c], or $\{\text{CH}_2\text{C}_6\text{H}_4\text{P}(\text{o-tolyl})_2\}$ [Figure 6d, 6e], have been described¹¹. Compounds with cyclometallation were isolated for every instance. Figure 6 shows representative architectures of cations of all such products. In each complex, L^1 once more forms a planar coordination between two thioether-donors and two donor atoms from the respective co-ligand.



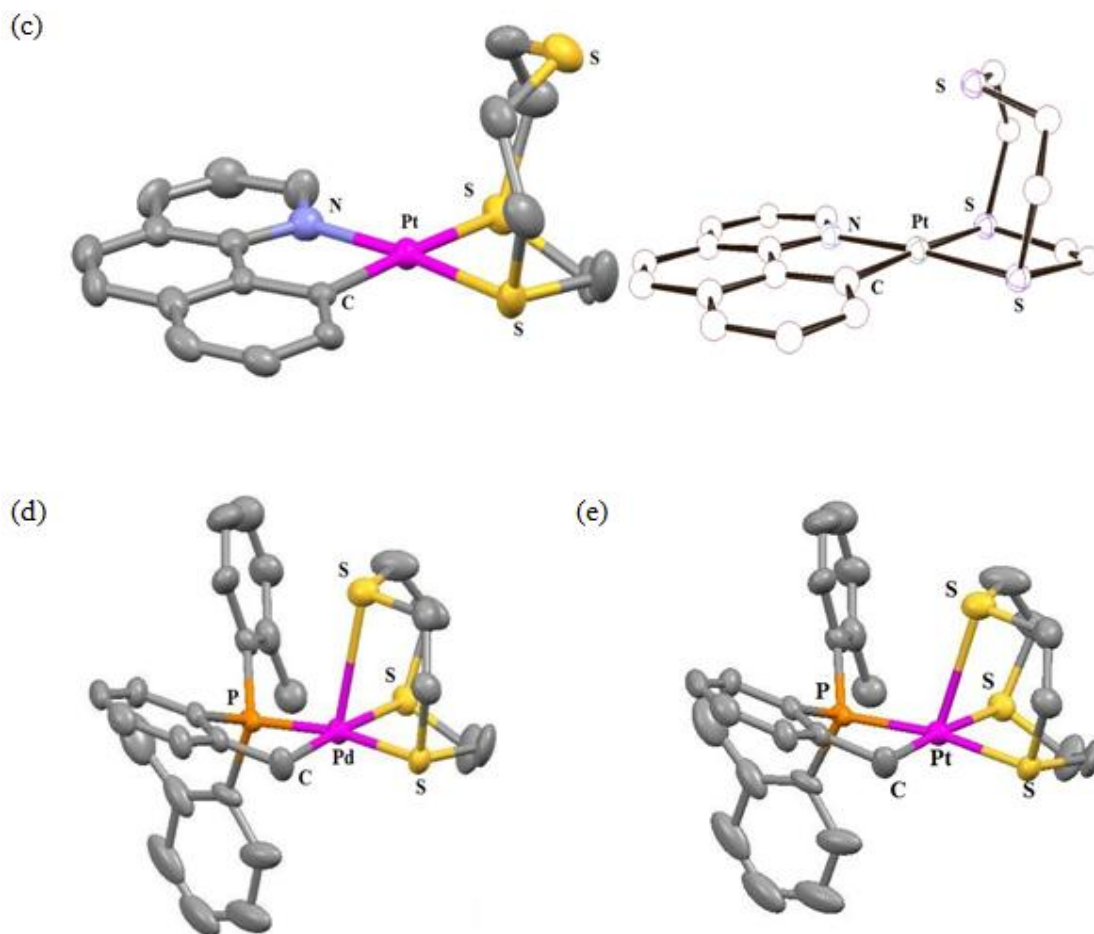


Figure 6

The axial M-S distance for all complexes is likewise greater than would be predicted for a typical metal-coordinate bonding, but it is still shorter than the total of the individual van der Waals radii. The structural framework of L^1 is disordered, providing the formation of two distinct types; *exo*-S-axial and *endo*-S-axial [Figure 6c], having *exo*-form constituting the predominant constituent. Investigations reveal that in these compounds the metal-bound L^1 ligand displays fluxional activity in CD_3NO_2 , as has been seen for similar species.

Additionally, Pt^{II} compounds of L^1 with two XPh_3 ($X = As$ or Sb) co-ligands as well as the similar compound $[Pt(L^1)(dpae)](PF_6)_2$ [$dpae = 1,2$ -bis(diphenylarsenio)ethane] were also produced. The following complexes are reported¹²: $[Pt(L^1)(AsPh_3)_2](PF_6)_2$ [Figure 7a], $[Pt(L^1)(AsPh_3)(Cl)](PF_6)$ [Figure 7c], $[Pt(L^1)(SbPh_3)_2](PF_6)_2$ [Figure 7b], $[Pt(L^1)(SbPh_3)(Cl)](PF_6)$ [Figure 7d], $[Pt(L^1)(dpae)](PF_6)_2$ [Figure 7f], and $[Pd(L^1)(dpae)](PF_6)_2$ [Figure 7e]. In all of those, the framework reveals that two S atom from L^1 are once more attached to the corresponding metal centers in a square planar configuration, jointly with two XPh_3 or the (bidentate) $dpae$ ligand, with the third S atom from L^1 holding an axial location. In Figure 7, the structures are displayed. In an additional investigation, it was shown that recrystallizing $[Pt(L^1)(SbPh_3)_3](PF_6)_2$ from nitromethane at room temperature results in the sudden production of $[Pt(L^1)(SbPh_3)(C_6H_5)](PF_6)$ ¹³ [Figure 7g].

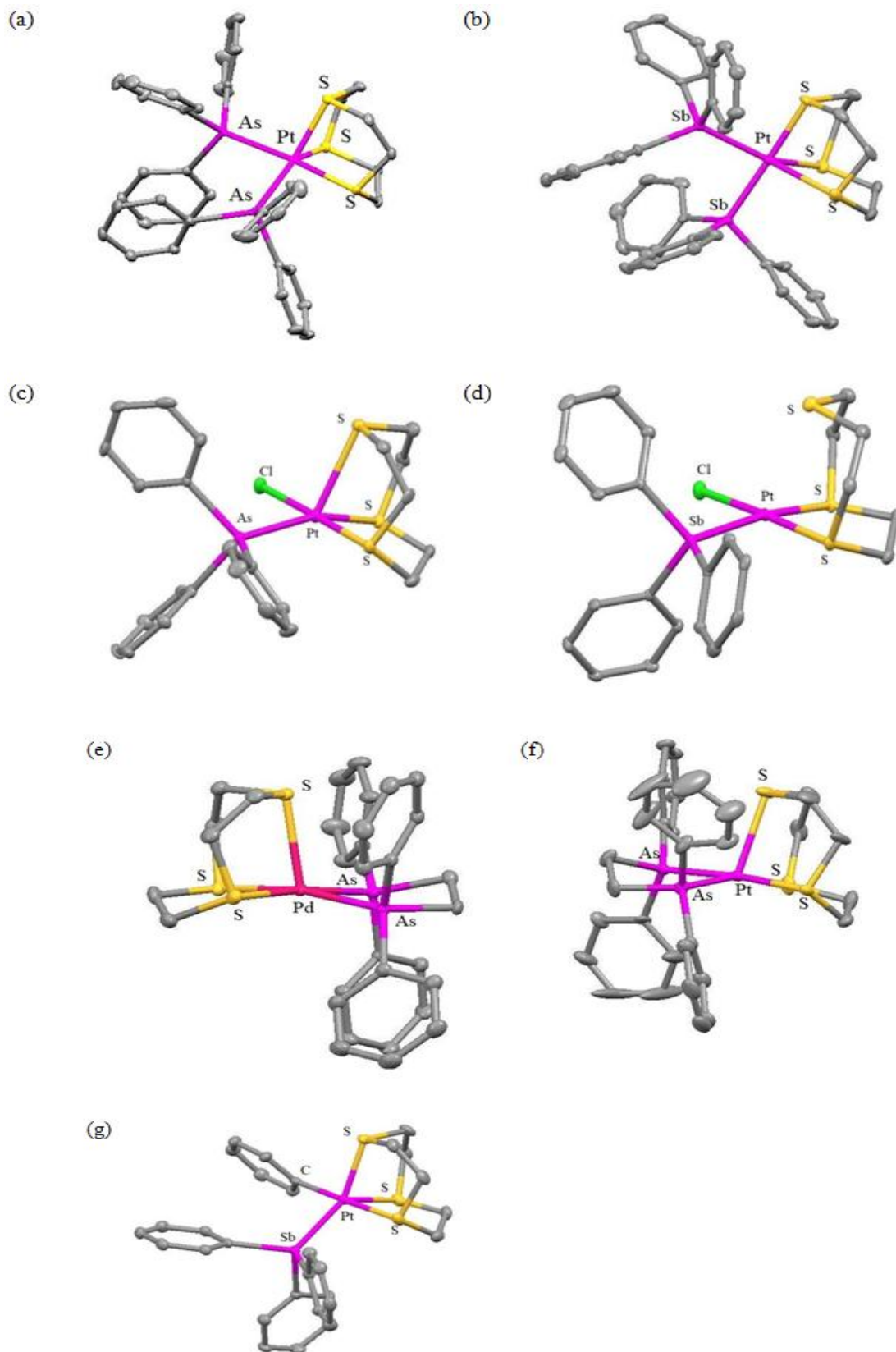


Figure 7

In the self-assembling process of a tetra Pt^{II} molecular square, [Pt(L¹)(bipy)]₄(OTf)₈, containing bipy (4,4-bipyridine) edges, it has been observed that four L¹ ligands are used as corner "capping" components¹⁴. Each L¹ ligand displays fluxional habits in solution. This is true for all "formally" 4-coordinate corners Pt^{II} centers. Figure 8 depicts the solid state structure of cation. It has four triflate anions occupying the square's hollow. Later, it was demonstrated that even though the aforementioned square is stable in nitromethane, it gradually changes into a new complex that is probably the respective metallo-triangle in acetonitrile. Several more metal thia crown compounds were also described in the context of the aforementioned investigation.

These comprised new Pd^{II} compound [{Pd(L¹)Cl₂}₂(pyrazine)](OTf)₂ [Figure 9d] and two Rh^{III} complexes, *cis*-[Rh(L⁴)Cl₂](PF₆) [Figure 9b] and *trans*-[Rh(L⁵)(H₂O)Cl](OTf)₂ [Figure 9c]. Also identified was a hybrid platinum(II) complex of the type [Pt(L¹)(CH₃CN)₂][Pt(L¹)₂](PF₆)₆ [Figure 9a]. These structures are shown in Figure 9. Only two S-donors are used by L¹ to coordinate the aforementioned Pd^{II} and Pt^{II} complexes, respectively, whereas the third S occupies an axial position with a longer proximity to the corresponding metal ions (2.9 Å for Pd and 3.0-3.1 Å for Pt)¹⁵.

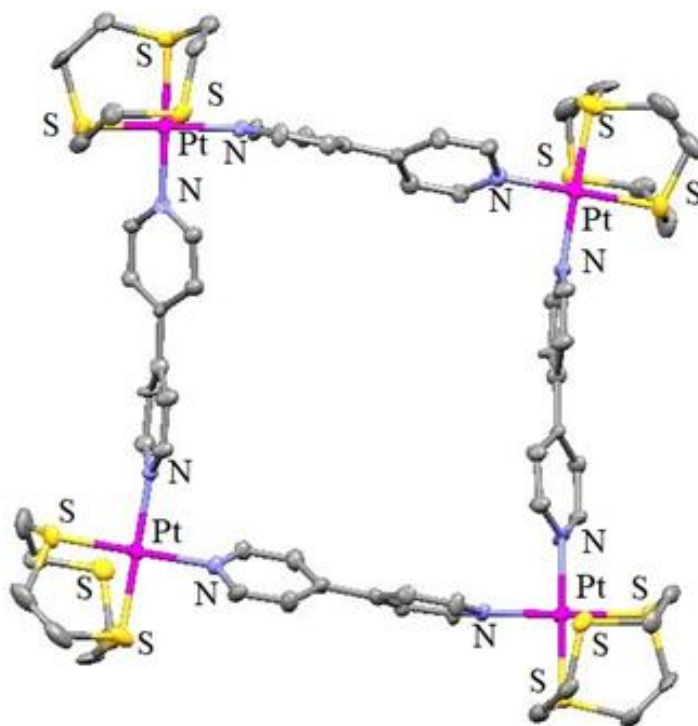


Figure 8

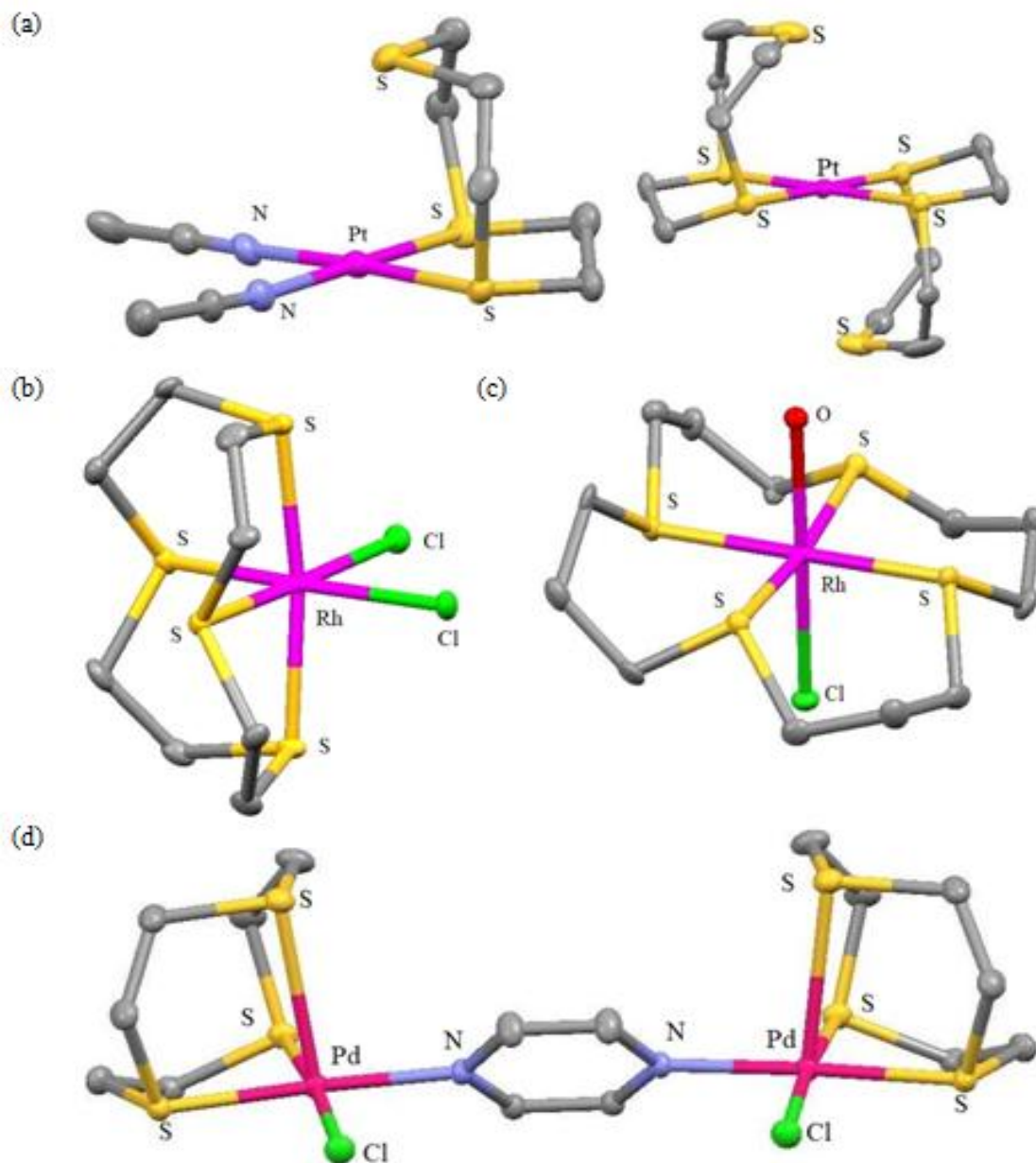


Figure 9

The $[\text{Ru}(\text{L}^1)(\text{glycino})\text{Cl}]$ compound was synthesized by reacting $[\text{Ru}(\text{L}^1)(\text{dmsO})\text{Cl}_2]^{16}$ (dmsO = dimethylsulfoxide) [Figure 10] with a small excess of glycine in the presence of a base. This compound possesses an octahedral geometry due to the glycino ligand coordinate in its typical (O,N)-bidentate form¹⁷. For 1:1 insertion in the cavity of cyclodextrin and similar substituted derivatives, this species serves as a guest. Physical studies confirm the presence of bound glycinate is in the cyclodextrin cavity.

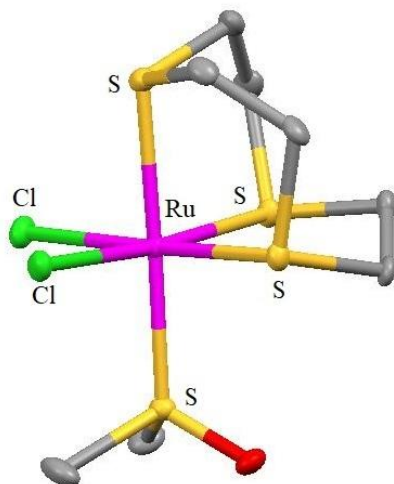
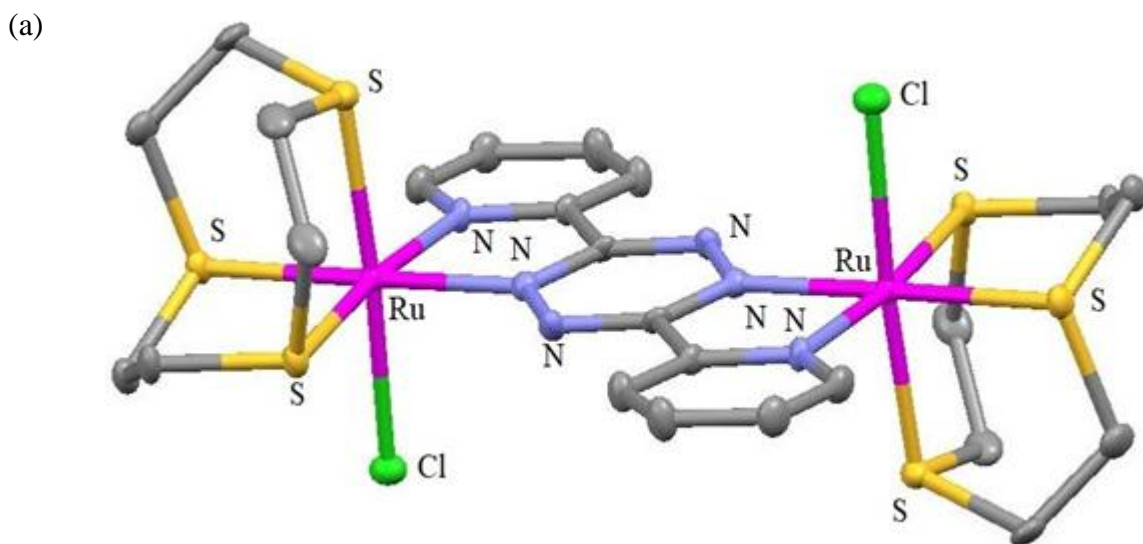


Figure 10

Electronic characteristics of bpta-bridged dinuclear compounds of the types $[(RuL)_2(bpta)](PF_6)_4$ [Figure 11b and 11c], [bpta = 3,6-bis(2-pyridyl)-1,2,4,5-tetrazine, $L = L^4$ or L^5], and $[(RuL^1Cl)_2(bpta)](PF_6)_2$ [Figure 11a] are affected by S-donor thiacycrown ligands¹⁸. These complexes were made by reacting bpta to the respective parent $[(Ru(S_4\text{-macrocycle})(dmsO)Cl)](PF_6)$ compound; Figure 11 depicts the bridging architecture of the final products. It was proposed that the redox and electrical characteristics of each compound portray the bonding behavior of the S donors in the corresponding S_4 -crowns.



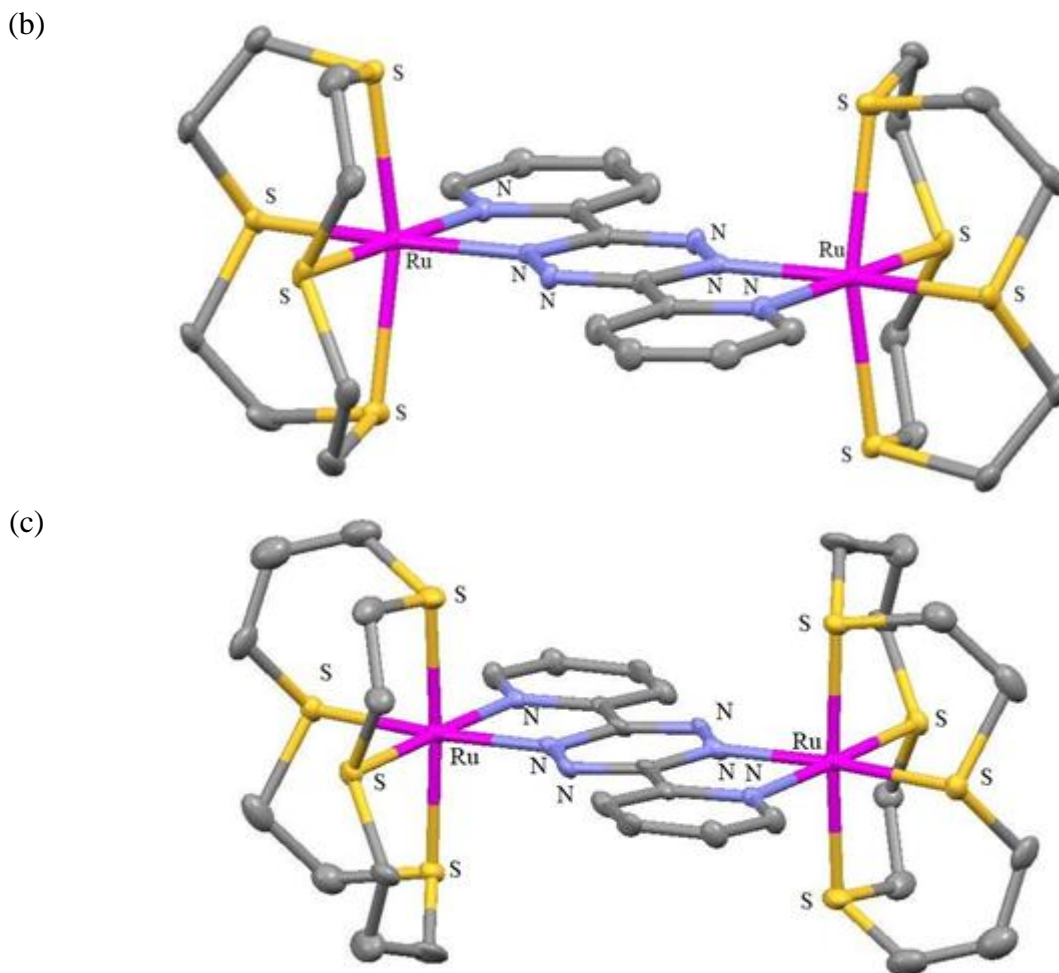
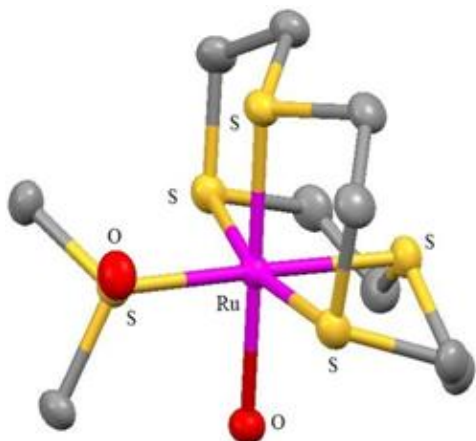


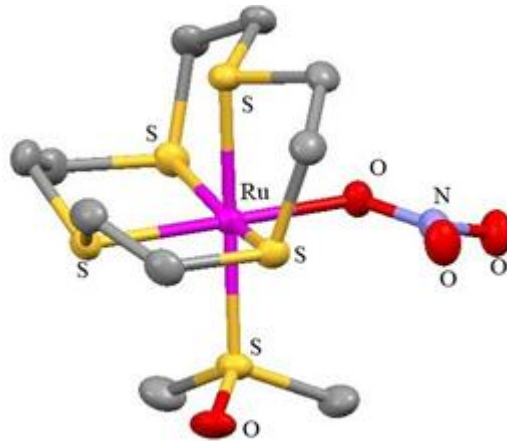
Figure 11

Using two moderately labile co-ligands like chloride, nitrate, water, or dimethyl sulfoxide, octahedral Ru^{II} compounds of the S₄-donor, L⁴ and L⁶ ligands were produced¹⁹. The chemical composition of the compounds are *cis*-[Ru(L⁴)(dmsO)(H₂O)](CF₃SO₃)₂ [Figure 12a], *cis*-[Ru(L⁴)(dmsO)(ONO₂)](NO₃) [Figure 12b], [Ru(L⁴)₂](CF₃SO₃)₂ [Figure 12c], *cis*-[Ru(L⁶)Cl₂] [Figure 12d], and *trans*-[Ru(L⁶)(dmsO)(H₂O)](CF₃SO₃)₂ [Figure 12e]. The L⁴ ring is too small to wrap Ru^{II}, yielding only *cis*- complexes, whereas the bigger macrocycle generates both *cis*- and *trans*- octahedral species. The pyrazine's (pyz) reaction with the compounds revealed that the anion found in the precursor affects the type of substance that is later separated. The compound [Ru(L⁴)(dmsO)Cl]Cl is *cis*-, pyz combines to form [(Ru(L⁴)Cl)₂(pyz)]Cl₂ [Figure 12f]. In a similar manner, pyz's interaction with *cis*-[Ru(L⁴)(dmsO)(ONO₂)](NO₃), produces the dinuclear compound [Ru(L⁴)(ONO₂)₂(pyz)](NO₃)₂. While *cis*-[Ru(L⁴)(dmsO)(H₂O)](CF₃SO₃)₂ generates the analogous bridging trinuclear compound [{*cis*-Ru(L⁴)(pyz)]₃](CF₃SO₃)₆ [Figure 12g].

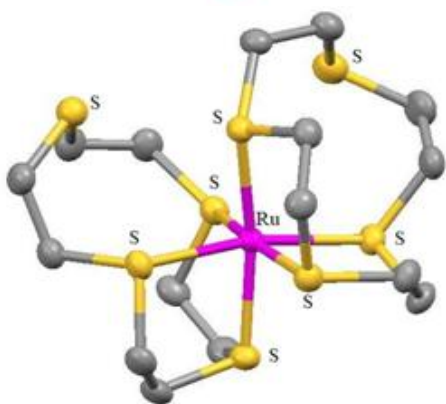
(a)



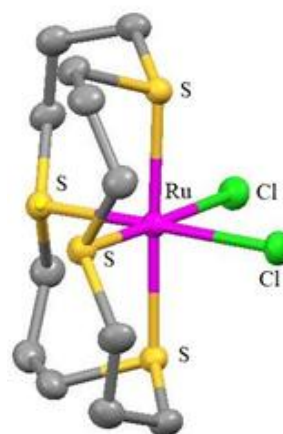
(b)



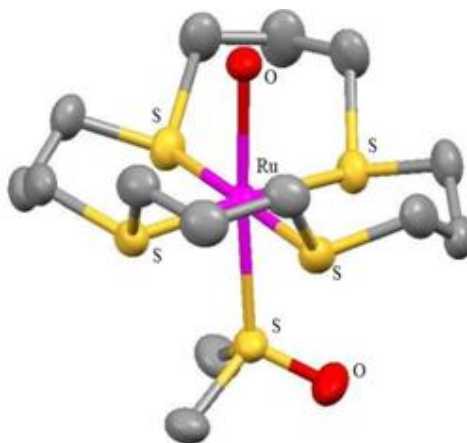
(c)



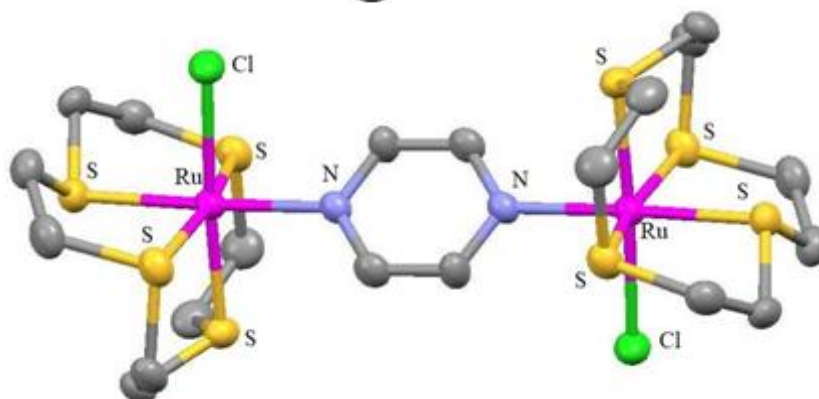
(d)



(e)



(f)



(g)

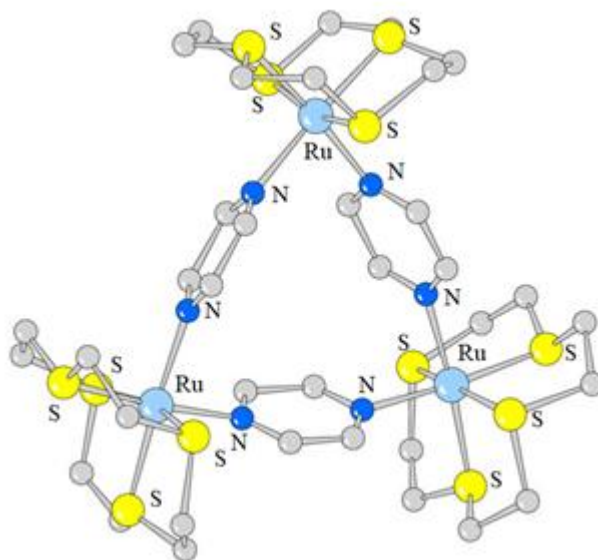
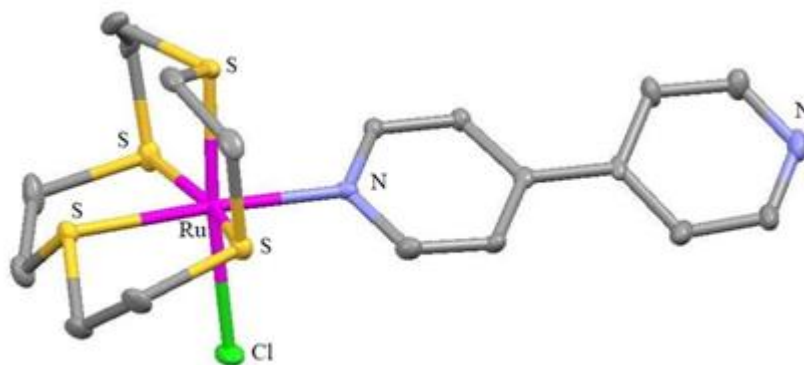


Figure 12

Both $[\text{Ru}(\text{L}^4)(\text{bpy})\text{Cl}]\text{Cl}$ [Figure 13a] and $[\{\text{Ru}(\text{L}^4)\text{Cl}\}_2(\text{bpy})](\text{PF}_6)_2$ [Figure 13b] ($\text{bpy} = 4,4\text{-bipyridine}$), constitute mixed ligand compounds²⁰. The Ru^{II} centers assume a distorted cis-octahedral coordinating architecture in each compound, binding to one N from bpy and chloride in addition to the S_4 -donor set of L^4 . Bipyridine serves as a connector among the metal centers in the second compound. The electrochemical findings in each situation support the existence of the $\text{Ru}^{\text{II}}/\text{Ru}^{\text{III}}$ couple's reversible one electron mechanism. Creutz-Taube ion analogues²¹ were prepared as nine fresh compounds that include pairs of $[\text{Ru}^{\text{II}}(\text{L})\text{Cl}]^+$ components ($\text{L} = \text{L}^4, \text{L}^5, \text{or } \text{L}^6$) connected by linear bis-monodentate linking N-donor ligands, pyrazine, 4,4-bipyridine, or 3,6-bis(4-pyridyl)-1,2,4,5-tetrazine. The coordinated S_4 -macrocycle's different ring sizes greatly affect the electronic delocalization throughout this set, although the Ru^{II} centers being linked to identical donor groups, according to the analysis of the inter valence charge transfer absorption patterns for the various compounds²². The $[\text{Ru}(\text{L}^7)\text{Cl}](\text{PF}_6)$ ²³ [Figure 14] architecture reveals that the cation has a deformed octahedral framework, with the chloride unit assuming the sixth/axial site and all five S-donors of L^7 linked in a square pyramidal way. Once more, this combination exhibits the $\text{Ru}^{\text{II}}/\text{Ru}^{\text{III}}$ couple's one electron redox activity in CH_3CN .

(a)



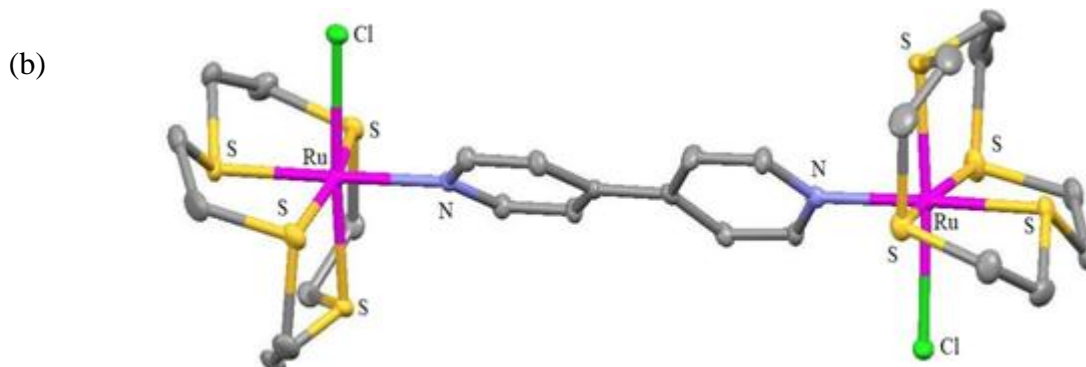


Figure 13

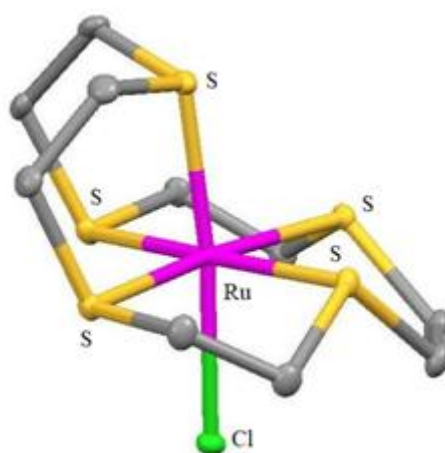


Figure 14

Numerous mixed-ligand Ru^{II} compounds of L^1 , L^4 and L^5 with two nicotinamide, isonicotinamide, or p-cyanobenzamide co-ligands; $[\text{Ru}(\text{L}^1)(\text{nicotinamide})_2\text{Cl}](\text{PF}_6)$ [Figure 15a], $[\text{Ru}(\text{L}^1)(\text{isonicotinamide})_2\text{Cl}](\text{PF}_6)$ [Figure 15b], $[\text{Ru}(\text{L}^4)(\text{nicotinamide})_2](\text{PF}_6)_2$ [Figure 15c], $[\text{Ru}(\text{L}^4)(\text{isonicotinamide})_2](\text{PF}_6)_2$, $[\text{Ru}(\text{L}^4)(\text{p-cyanobenzamide})_2](\text{PF}_6)_2$, $[\text{Ru}(\text{L}^5)(\text{nicotinamide})_2](\text{PF}_6)_2$ [Figure 15d], $[\text{Ru}(\text{L}^5)(\text{isonicotinamide})_2](\text{PF}_6)_2$ and $[\text{Ru}(\text{L}^5)(\text{p-cyanobenzamide})_2](\text{PF}_6)_2$ [Figure 15e], in order that every single unit has amide ($-\text{CONH}_2$) functionalities that are positioned peripherally and are accessible for generating hydrogen bonds²⁴. These serve as the foundation for the construction of H-bonded solids. X-Ray diffraction was used for analysing six of them. While two of these systems produce networks using amide-anion $\text{N-H}\cdots\text{F}$ H-bonds connecting the complex components, four of these compounds build networks using amide-amide $\text{N-H}\cdots\text{O}$ H-bonds. Figure 16 represents the H-bonded networks. Along the series, a shift from 1D to 2D architecture was seen.

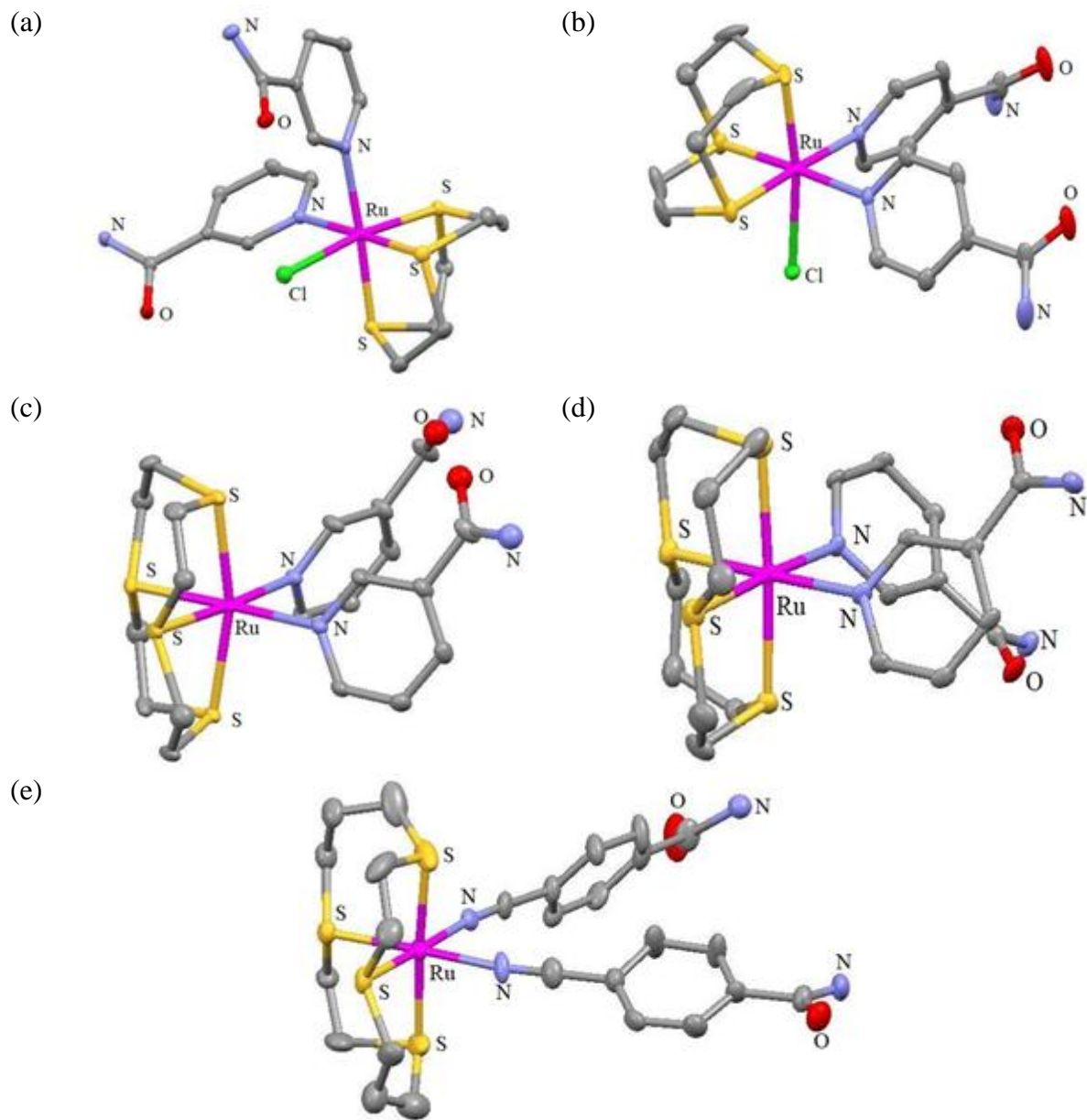
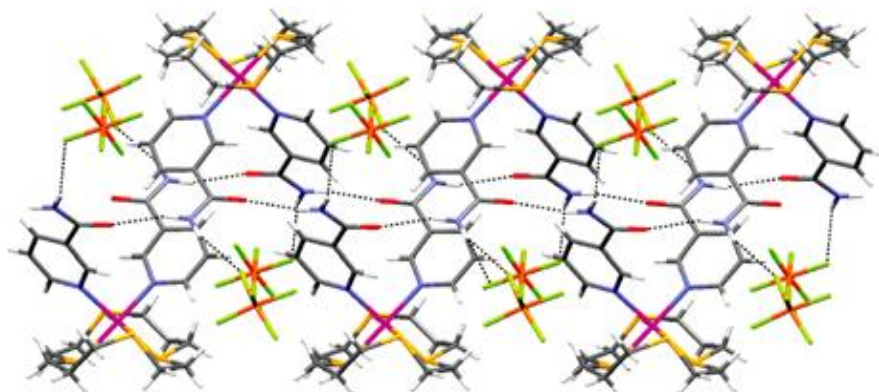
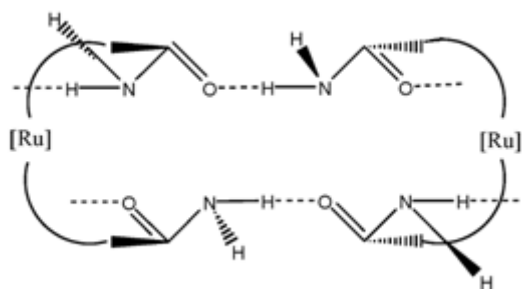
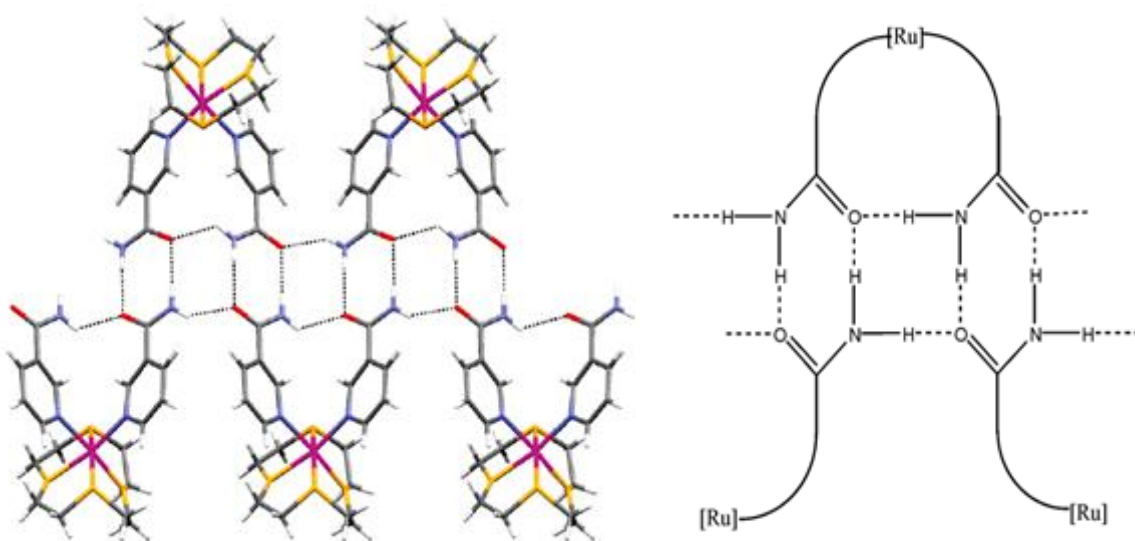


Figure 15

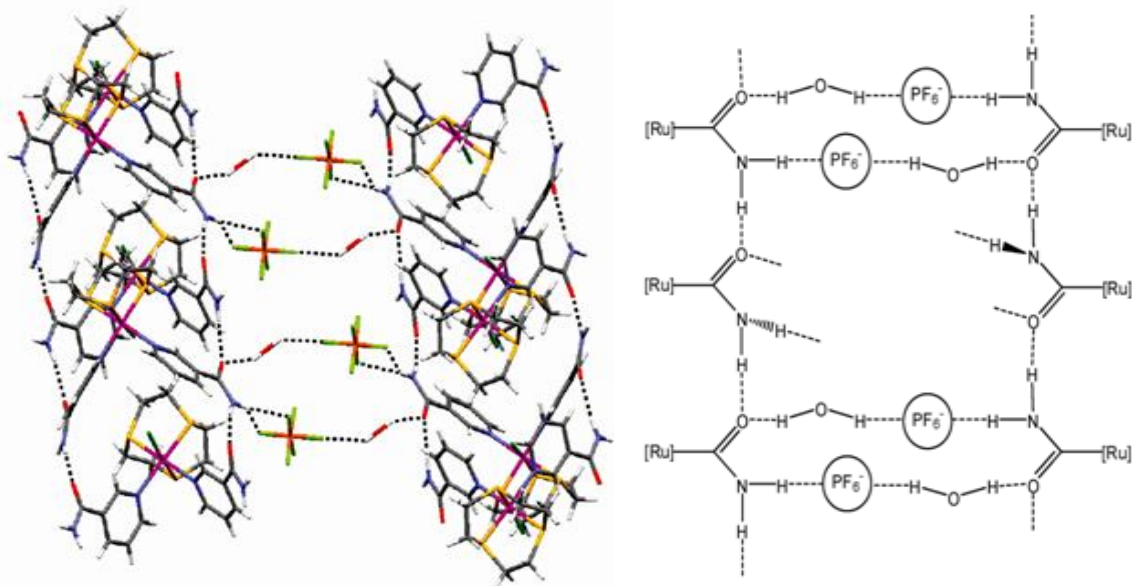




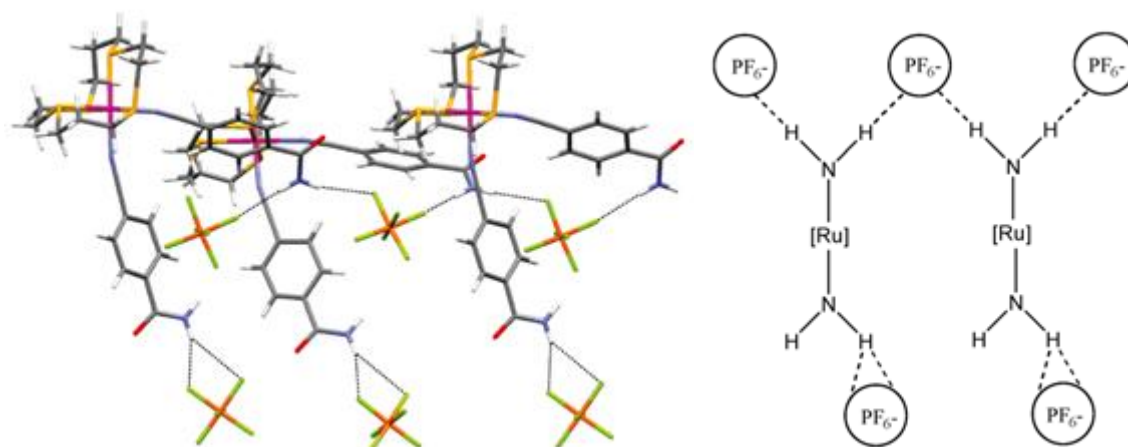
Hydrogen-bonded double chain linking $[\text{Ru}(\text{L}^5)(\text{nicotinamide})_2]^{2+}$ cations in $[\text{Ru}(\text{L}^5)(\text{nicotinamide})_2](\text{PF}_6)_2$ and its representation



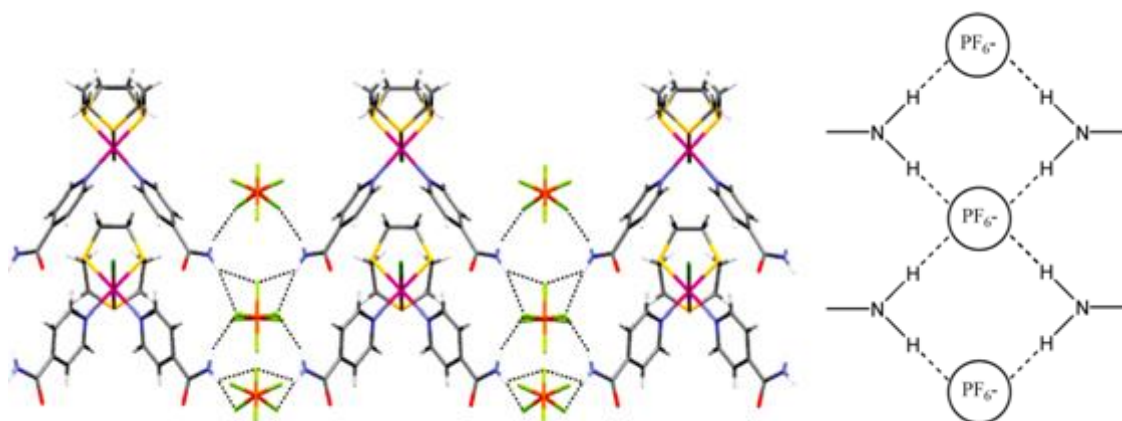
Hydrogen-bonded double chain linking $[\text{Ru}(\text{L}^4)(\text{nicotinamide})_2]^{2+}$ cations in $[\text{Ru}(\text{L}^4)(\text{nicotinamide})_2](\text{PF}_6)_2$ and its representation



Hydrogen-bonded layers containing solvent/anion-expanded amide tapes of $[\text{Ru}(\text{L}^1)(\text{nicotinamide})_2\text{Cl}](\text{PF}_6)$ and its representation



Amide-Anion Hydrogen-Bonded Chain in $[\text{Ru}(\text{L}^5)(\text{p-cyanobenzamide})_2](\text{PF}_6)_2$ and its representation

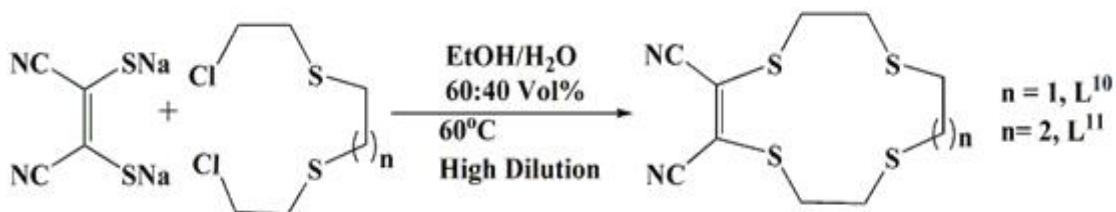


2D hydrogen-bonded structure of $[\text{Ru}(\text{L}^1)(\text{isonicotinamide})_2\text{Cl}](\text{PF}_6)$ and its representation

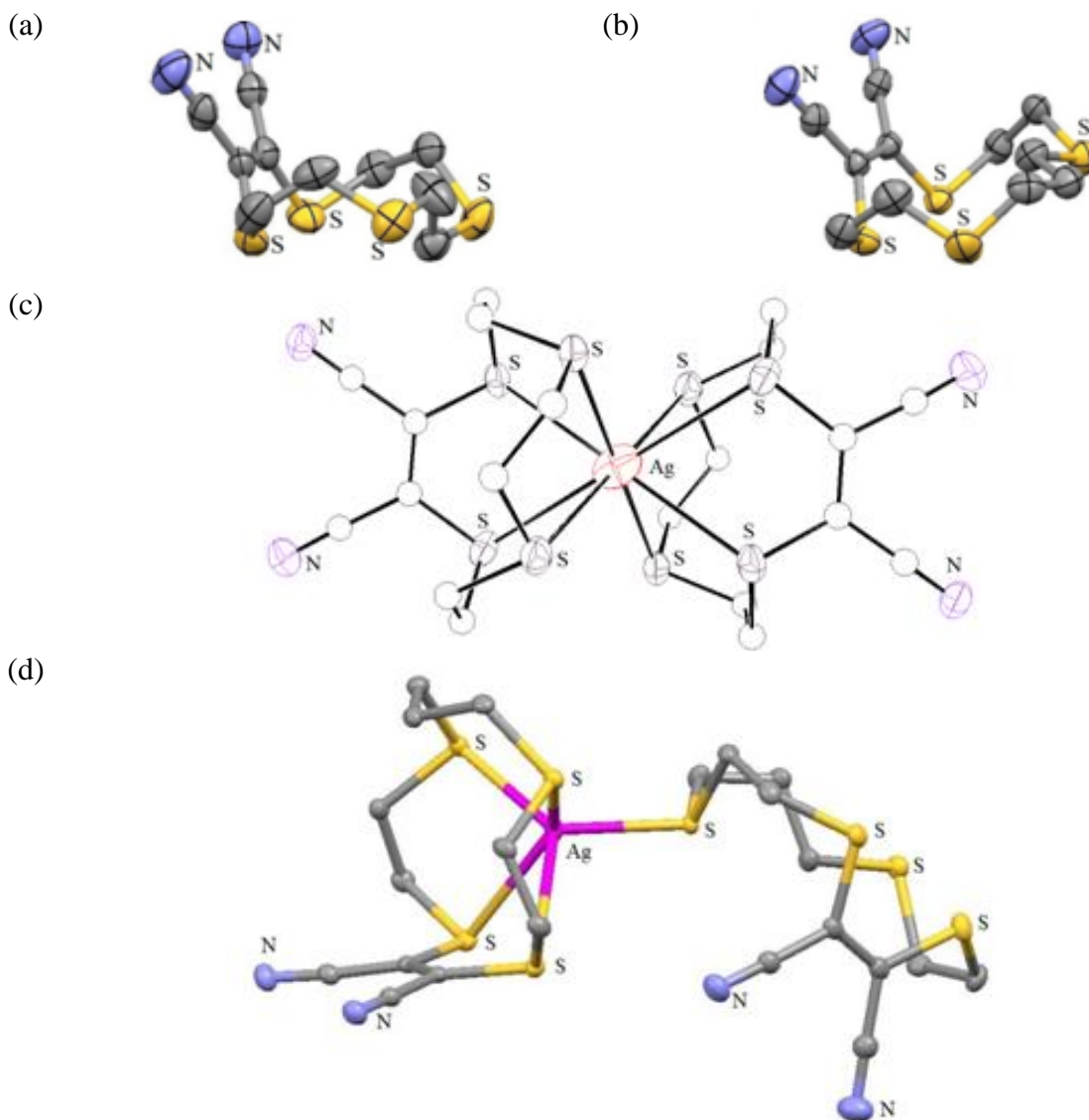
Figure 16

Two of the S atoms are more likely to be pre-oriented *endo*- in relation to the macrocyclic cavity for every scenario when the maleonitrile component is present in the L^{10} and L^{11} macrocycles²⁵. Their crystal structures are shown in Figure 17a and 17b, respectively. The ligands are prepared by the procedure shown in Scheme 2. The following complexes were synthesized $[\text{Ag}(\text{L}^{10})_2]\text{BF}_4$ [Figure 17c], $[\text{Ag}(\text{L}^{10})_2](\text{PF}_6)$, $[\text{Ag}(\text{L}^{10})](\text{BF}_4)$, $[\text{Ag}(\text{L}^{10})](\text{PF}_6)$, $[\text{Ag}_2(\text{L}^{10})_3](\text{BF}_4)_2[\text{Ag}(\text{L}^{11})_2](\text{BF}_4)$ [Figure 17d], $[\text{Ag}(\text{L}^{11})_2](\text{PF}_6)$, $[\text{Ag}(\text{L}^{11})](\text{BF}_4)$, $[\text{Ag}(\text{L}^{11})](\text{PF}_6)$ and $[\text{Ag}_2(\text{L}^{11})_3](\text{PF}_6)_2$ [Figure 17e]. The bis-ligand combination $[\text{Ag}(\text{L}^{10})_2]^+$, which has a sandwich like structure as well as S_8 -coordination (distorted cubic shape), is produced when the 12-membered L^{10} interacts with Ag^{I} salts. Conversely, an important modification in the coordination tendency with Ag^{I} occurs when the S_4 macrocycle's ring dimension is increased to 13 atoms to produce L^{11} . In this instance, the Ag^{I} complexes $[\text{Ag}(\text{L}^{11})_2]\text{BF}_4$ and $[\text{Ag}_2(\text{L}^{11})_3](\text{PF}_6)$ were separated. Producing distorted square pyramidal coordinating environment, the $\text{Ag}(\text{I})$ in $[\text{Ag}(\text{L}^{11})]^+$ is attached to four S atoms from one L^{11} and one S from a second L^{11} , functioning as a monodentate ligand. $[\text{Ag}_2(\text{L}^{11})_3](\text{PF}_6)_2$ cation is made up of two $[\text{Ag}(\text{L}^{11})]^+$ components. In every

component, the metal centre is coordinated with four S atoms of L¹¹ type. A second L¹¹ macrocycle that combines in a bis-monodentate fashion using *cis*-S atoms connects the metal centres in both units. This allows each Ag^I centre to attain 5-coordination and exhibit a distorted square pyramidal structure. The structures are shown in Figure 17.



Scheme 2



(e)

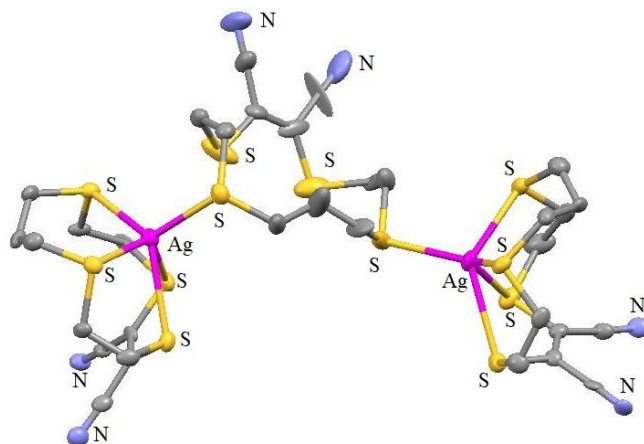
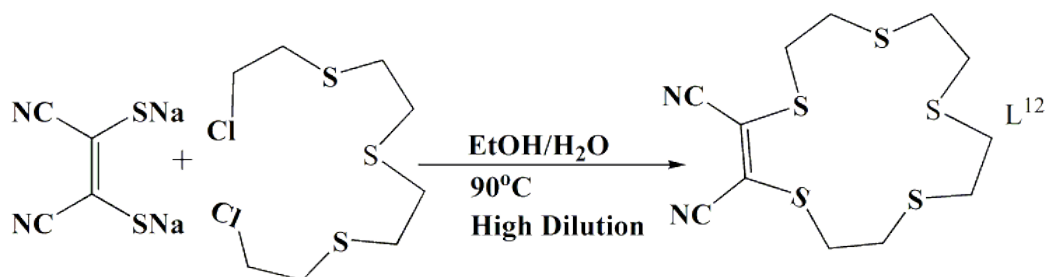


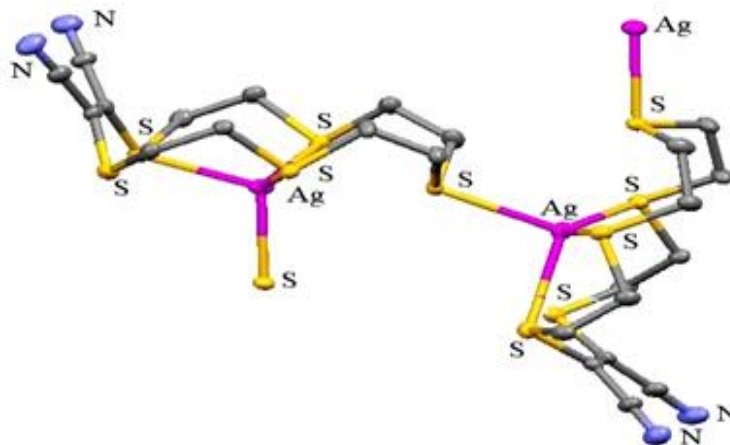
Figure 17

In an additional investigation, Hg^{II} was used to generate compounds containing L^{10} and L^{11} . For instance, $\text{Hg}(\text{ClO}_4)_2$ interacts with L^{11} to produce a dinuclear compound $[\text{Hg}_2(\text{L}^{11})_3](\text{ClO}_4)_4$, that has macrocycle bridges and shares structural similarities with the dinuclear Ag^{I} compound described previously²⁶. Complexes of category HgX_2L ($\text{X} = \text{Chloride}$ or iodide and $\text{L} = \text{L}^{10}$ or L^{11}) were produced using Hg^{II} chloride and iodide. In the investigation, the equivalent 15-membered, S_5 maleonitrile counterpart L^{12} was also synthesised. This ligand generates a 1:1 (metal: ligand) compound of type $[\text{Ag}(\text{L}^{12})]\text{X}$ ($\text{X} = \text{ClO}_4^-$ [Figure 18a] or BF_4^- [Figure 18b]) when combined with Ag^{I} .

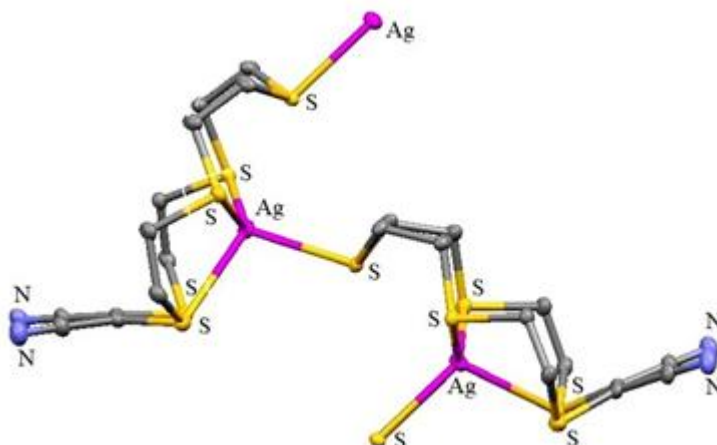


Scheme 3

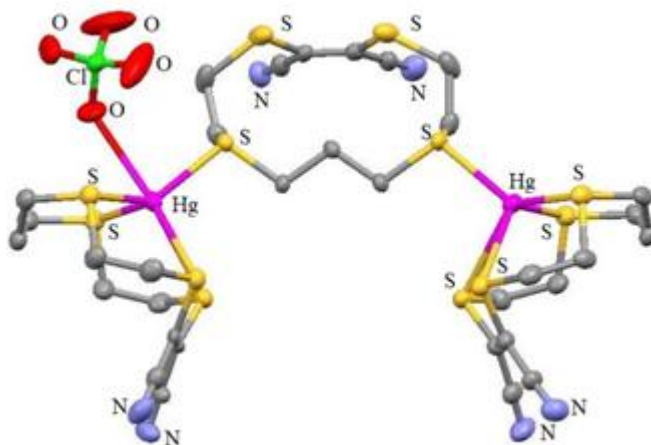
(a)



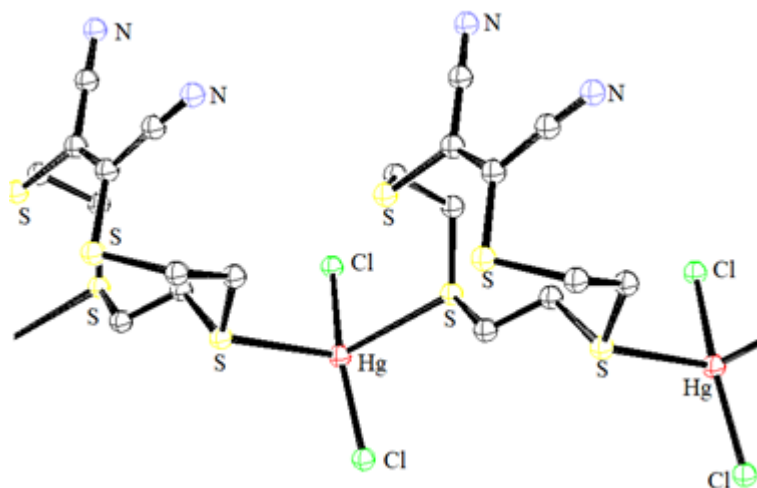
(b)



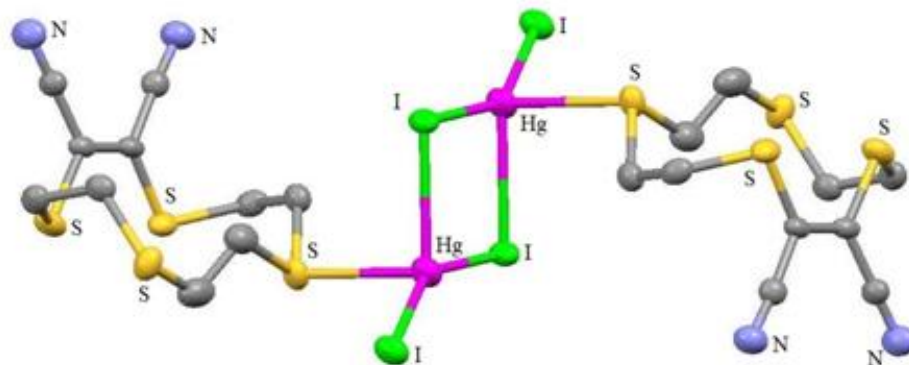
(c)



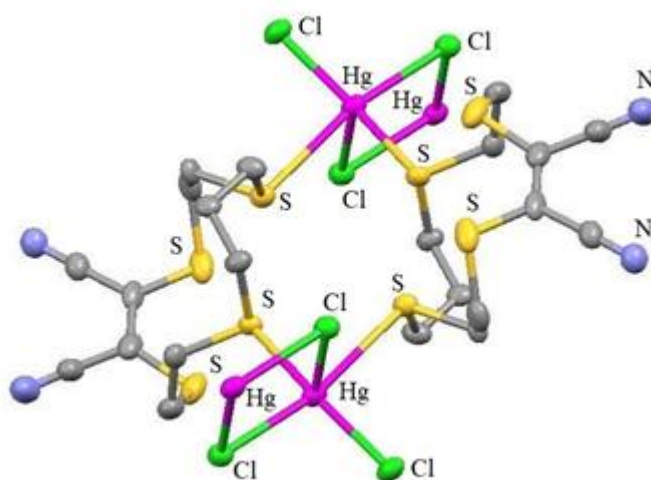
(d)



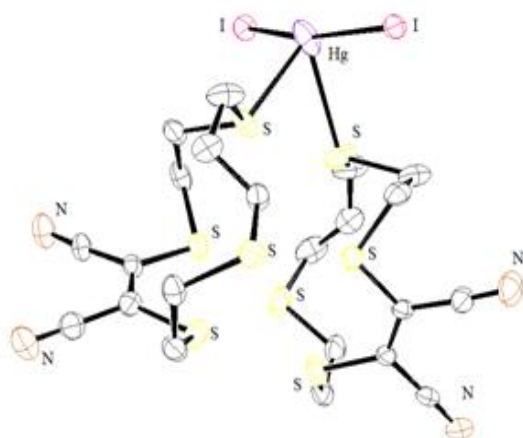
(e)



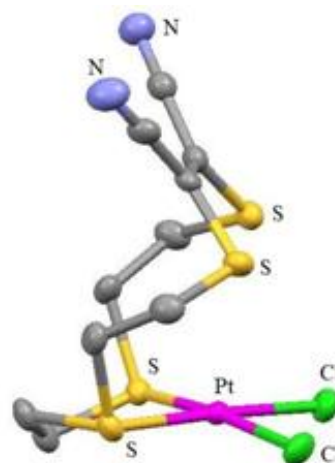
(f)



(g)



(h)



(i)

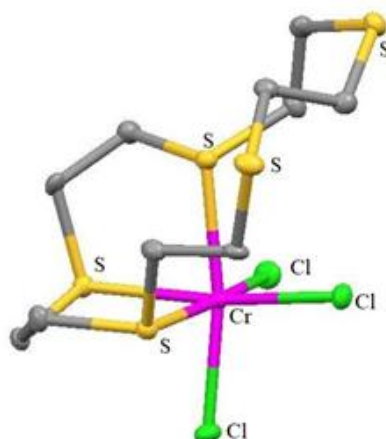


Figure 18

In every compound, the cation exhibits zigzag chain architecture. L^{12} was synthesized as in scheme 3. The following compounds [Figure 18] are reported; $[Ag(L^{12})]ClO_4$ [Figure 18a], $[Ag(L^{12})]BF_4$ [Figure 18b], $[Hg_2(L^{11})_3](ClO_4)_4$ [Figure 18c], $[HgCl_2(L^{10})]$ [Figure 18d], $[HgI_2(L^{10})]$ [Figure 18e], $[HgCl_2(L^{11})]$ [Figure 18f], $[HgI_2(L^{11})_2]$ [Figure 18g] and $[PtCl_2(L^{10})]$ [Figure 18h].

In an additional investigation, it was shown that the S_5 -donor macrocycle L^7 can interact with Cr^{III} to create a deformed octahedral compound $[Cr(L^7)Cl_3]$ ²⁷ [Figure 18i] where this ligand binds facially by three of its S-donors, while the rest coordination sites filled by three chloride ligands. Two L^7 S-donors continue to be acting non-coordinated.

As potential equivalents of the "blue" copper proteins, 21-membered S_6 -donor ligand L^{13} 's [Figure 19a] Cu^I/Cu^{II} compounds was studied²⁸. The flexible nature of this macrocycle was thought to have contributed to the development of an adequate tetrahedral configuration for Cu^I , which is why this macrocycle was found to prefer coupling to Cu^I over Cu^{II} by a margin of twelve orders of scale. The Cu^I complex's $[Cu(L^{13})(ClO_4)]$ [Figure 19b] solid state framework reveals that four S donors of L^{13} bind in a distorted tetrahedral configuration around the Cu^I centre, while the other two donors in the surrounding ring are unbound. Thiamacrocycles have the unique capacity to stabilise particular metals at their lower oxidation states²⁹.

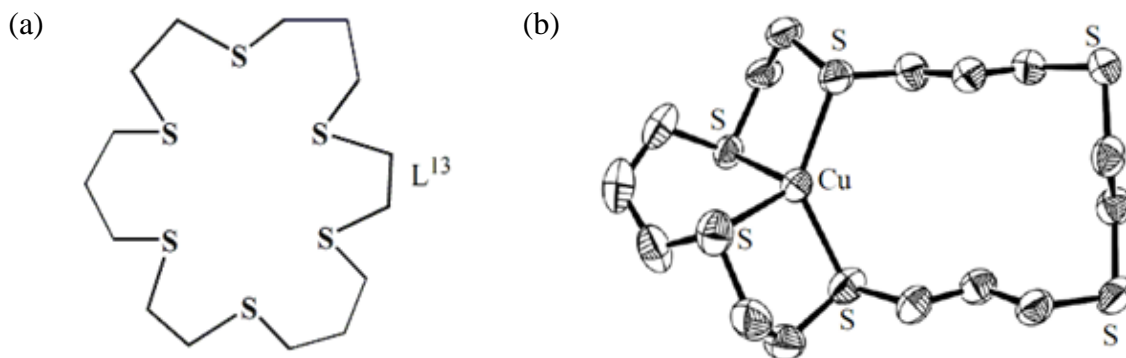


Figure 19

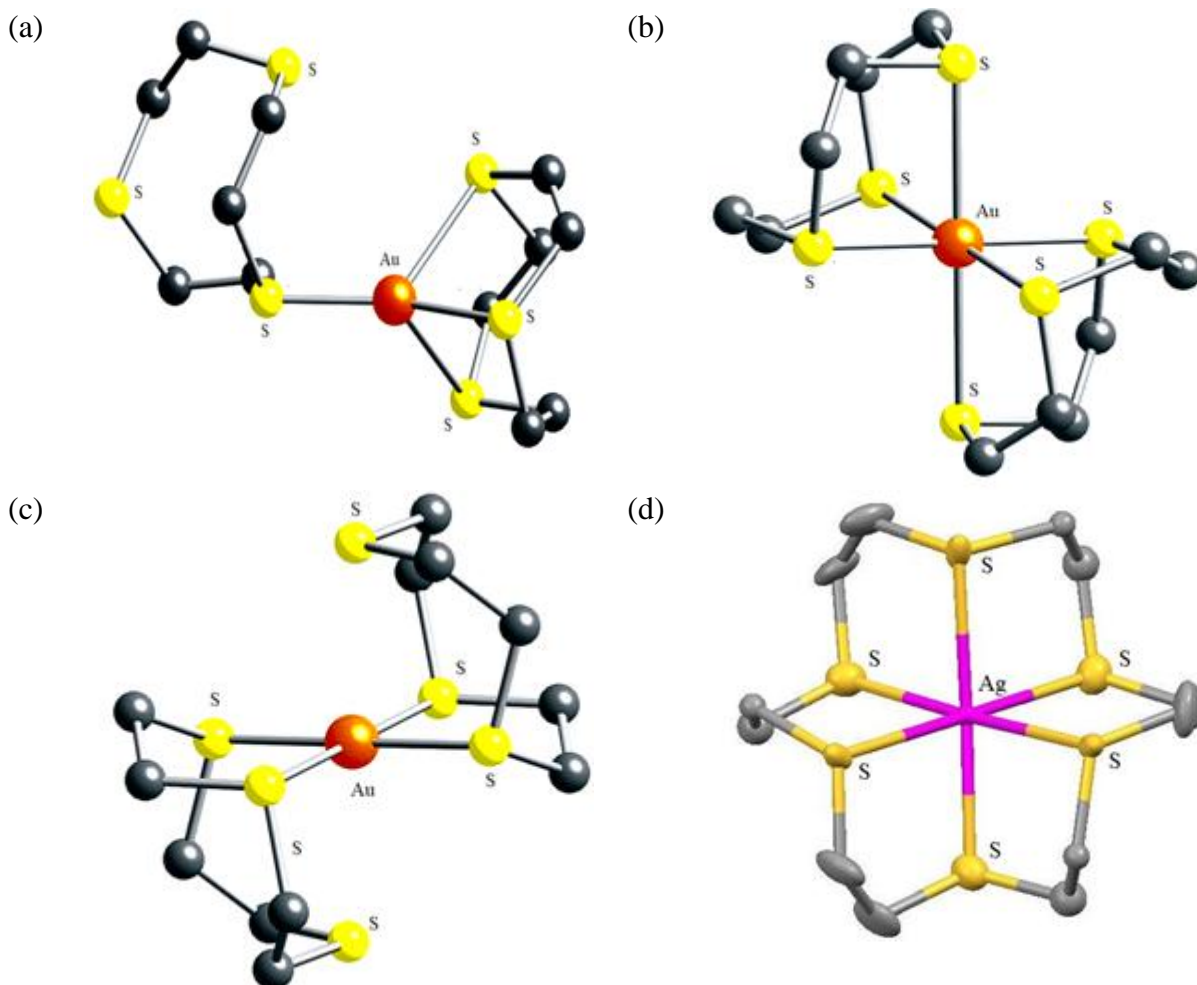


Figure 20

In the X-Ray structures of cations of the complexes $[\text{Au}(\text{L}^1)_2]^{1+/2+/3+}$, the binding of Au^{I} , Au^{II} , and Au^{III} centres [Figure 20a, 20b and 20c, respectively] have been described^{30,31}. Thorough analysis of $[\text{Au}^{\text{II}}(\text{L}^1)_2](\text{BF}_4)_2$ and $[\text{Ag}^{\text{II}}(\text{L}^8)](\text{ClO}_4)_2$'s electronic characteristics were reported³² [Figure 20d]. Second compound was the first of this type of Ag^{II} entities to involve complete thioether donor binding and was structurally characterized. The distances between the different Ag-S bonds are smaller than they are in the similar Ag^{I} octahedral compound. Thioether donors serve a “non-innocent” role in maintaining the theoretically +2 oxidation levels that these entities exhibit.

III. CONCLUSION

Over the years, chemistry of only thioether containing macrocycles have developed to a great extent, credit goes to their vast, yet interesting coordination chemistry. In this chapter, several such ligands are discussed along with their reported metal complexes and brief discussion of their molecular structural frameworks have also been done both for transition as well as non-transition metal ions, briefly.

REFERENCE

- [1] C.J. Pedersen, "Cyclic polyethers and their complexes with metal salts", *J. Am. Chem. Soc.*, Vol. 89, pp. 7017–7036, 1967.
- [2] (a) J.M. Lehn, "Design of organic complexing agents Strategies towards properties", *Struct. Bond. (Berl.)* Vol. 16, pp. 1-69, 1973. (b) J.M. Lehn, "Supramolecular Chemistry—Scope and Perspectives Molecules, Supermolecules, and Molecular Devices (Nobel Lecture)", *Angew. Chem. Int. Ed. Engl.*, Vol. 27, pp. 89-112, 1988.
- [3] D.J. Cram, "The Design of Molecular Hosts, Guests, and Their Complexes (Nobel Lecture)", *Angew. Chem. Int. Ed. Engl.*, Vol. 27, pp. 1009-1020, 1988.
- [4] (a) B.M. Rambo, J.L. Sessler, "Oligopyrrole Macrocycles: Receptors and Chemosensors for Potentially Hazardous Materials", *Chem. Eur. J.* Vol. 17, pp. 4946-4959, 2011. (b) E. Tamanini, K. Flavin, M. Motevalli, S. Piperno, L.A. Gheber, M.H. Todd, M. Watkinson, "Cyclam-Based "Clickates": Homogeneous and Heterogeneous Fluorescent Sensors for Zn(II)" *Inorg. Chem.*, Vol. 49, pp. 3789-3800, 2010, (c) M.C. Aragoni, M. Arca, A. Bencini, A.J. Blake, C. Caltagirone, G. De Filippo, F.A. Devillanova, A. Garau, T. Gelbrich, M.B. Hursthouse, F. Isaia, V. Lippolis, M. Mameli, P. Mariani, B. Valtancoli, C. Wilson, "Tuning the Selectivity/Specificity of Fluorescent Metal Ion Sensors Based on N₂S₂ Pyridine-Containing Macrocyclic Ligands by Changing the Fluorogenic Subunit: Spectrofluorimetric and Metal Ion Binding Studies", *Inorg. Chem.*, Vol. 46, pp. 4548-4559, 2007.
- [5] L.F. Lindoy, "The Chemistry of Macrocyclic Complexes", Cambridge University Press, Cambridge, UK, pp. 1–269, 1989.
- [6] L.F. Lindoy, K.-M. Park, S.S. Lee, "Metals, macrocycles and molecular assemblies – macrocyclic complexes in metallo-supramolecular chemistry", *Chem. Soc. Rev.*, Vol. 42, pp. 1713-1727, 2013.
- [7] (a) A.J. Barton, N. J. Hill, W. Levason and G. Reid, "Synthesis and Structural Properties of the First Macrocyclic Selenoether Complex of Arsenic(III): A Rare Example of Exo and Endo Coordination in a Single Species", *J. Am. Chem. Soc.* Vol. 123, pp. 11801-11802, 2001. (b) R.E. Wolf, J.R. Hartman, J.M.E. Storey, B.M. Foxman, S.R. Cooper, "Crown thioether chemistry: structural and conformational studies of tetrathia-12-crown-4, pentathia-15-crown-5, and hexathia-18-crown-6. Implications for ligand design", *J. Am. Chem. Soc.*, Vol. 109, 4328-4335, 1987.
- [8] (a) M.L. Helm, L.L. Hill, J.P. Lee, D. G. Van Derveer and G. J. Grant, "Cadmium-113 NMR studies on homoleptic complexes containing thioether ligands: the crystal structures of [Cd([12]aneS₄)₂](ClO₄)₂, [Cd([18]aneS₄N₂)](PF₆)₂ and [Cd([9]aneS₃)₂](PF₆)₂", *Dalton Trans.*, Issue 29, pp. 3534-3543, 2006. (b) J.P. Lee, G.J. Grant and B.C. Noll, "Bis(1,4,7-trithiacyclononane)nickel(II) bis(tetrafluoroborate) nitromethanedisolvate", *Acta Crystallogr., Sect. E: Struct. Rep. Online*, Vol. 67, pp. M1417-M1418, 2011.
- [9] D.R. Allan, A.J. Blake, D.G. Huang, T. J. Prior and M. Schröder, "High pressure co-ordination chemistry of a palladium thioether complex: pressure versus electrons", *Chem. Comm.*, Issue 39, pp. 4081-4083, 2006.
- [10] (a) S. C. Rawle, G. A. Admans and S. R. Cooper, "Crown thioether chemistry. Synthesis and structural investigation of 1,5,9-trithiacyclododecane (trithia-12-crown-3) and its copper(II) chloride adduct", *J. Chem. Soc., Dalton Trans.*, Issue 1, pp. 93-96, 1988. (b) W. Rosen and D. H. Busch, "Octahedral nickel(II) complexes of some cyclic polyfunctional thioethers", *Inorg. Chem.* Vol. 9, pp. 262-265, 1970.
- [11] D.E. Janzen, D.G. Van Derveer, L.F. Mehne, D.A.D. Silva, J.L. Bredas and G.J. Grant, "Cyclometallated Pt(II) and Pd(II) complexes with a trithiacrown ligand", *Dalton Trans.* Issue 14, pp. 1872-1882, 2008.
- [12] G.J. Grant, D. A. Benefield and D.G. VanDerveer, "ThiacrownPt^{II} complexes with group 15 donor ligands: pentacoordination in Pt(II) complexes", *Dalton Trans.*, Issue 49, pp. 8605-8615, 2009.
- [13] G.J. Grant, D. A. Benefield and D.G. VanDerveer, "Antimony–Carbon bond activation in a Pt(II) complex: The crystal structure of [Pt(9S3)(SbPh₃)(Ph)](PF₆)-CH₃NO₂", *J. Organomet. Chem.*, Vol. 695, pp. 634-636, 2010.
- [14] D.E. Janzen, K.N. Patel, D.G. VanDerveer, G.J. Grant, "Synthesis and structure of a platinum(II) molecular square incorporating four fluxional thiacycrown ligands: The crystal structure of [Pt₄([9]aneS₃)₄(4,4'-bipy)₄](OTf)₈", *Chem. Commun.*, Issue 33, pp. 3540-3542, 2006.
- [15] G.J. Grant, R.D. Naik, D.E. Janzen, D. A. Benefield and D.G. VanDerveer, "Platinum group metal thiacycrown complexes as precursors for self-assembly reactions", *Supramol. Chem.* Vol. 22, pp. 109-121, 2010.
- [16] J. Marques, T.M. Braga, F.A.A. Paz, T.M. Santos, M.F. S. Lopes and S. S. Braga, "Cyclodextrins improve the antimicrobial activity of the chloride salt of Ruthenium(II) chloro-phenanthroline-trithiacyclononane", *BioMetals*, Vol. 22, pp. 541-556, 2009.

- [17] J. Marques, T.M. Santos, M. P. Marquesm and S.S. Braga, "A glycine ruthenium trithiacyclononane complex and its molecular encapsulation using cyclodextrins", *Dalton Trans.*, Issue44, pp. 9812-9819, 2009.
- [18] M. Newell, J.D. Ingram, T.L. Easun, S.J. Vickers, H. Adams, M. D. Ward and J.A.Thomas, "Structure and Properties of Dinuclear $[Ru^{II}([n]aneS_4)]$ Complexes of 3,6-Bis(2-pyridyl)-1,2,4,5-tetrazine", *Inorg. Chem.* Vol. 45, pp. 821-827, 2006.
- [19] E. Zangrando, N. Kulisic, F. Ravalico, I. Bratsos, S. Jedner, M. Casanova and E.Alessio, "New ruthenium(II) precursors with the tetradentatesulfurmacrocycletetrathiacyclododecane ([12]aneS4) and tetrathiacyclohexadecane ([16]aneS4) for the construction of metal-mediated supramolecular assemblies" *Inorg. Chim. Acta*, Vol. 362, pp. 820-832, 2009.
- [20] D.E. Janzen, W.N. Chen, D.G. VanDerveer, L. F. Mehne and G.J. Grant, "Synthesis and structural studies of ruthenium(II) 12S4 complexes with 4,4'-bipyridine: The crystal structures of $[Ru(12S4)(bpy)Cl](Cl) \cdot H_2O$ and $\{[Ru(12S4)Cl]_2-\mu-(bpy)\}(PF_6)_2 \cdot 2CH_3CN$ " *Inorg. Chem. Commun.* Vol. 9, pp. 992-995, 2006.
- [21] C. Creutz and H. Taube, "Binuclear complexes of ruthenium amines", *J. Am. Chem. Soc.* Vol. 895, pp. 1086-1094, 1973.
- [22] H. Adams, P.J. Costa, M. Newell, S.J. Vickers, M. D. Ward, V. Felix and J.A. Thomas, "Mixed Valence Creutz-Taube Ion Analogues Incorporating Thiocrowns: Synthesis, Structure, Physical Properties, and Computational Studies", *Inorg. Chem.*, Vol. 47, pp. 11633-11643, 2008.
- [23] D.E. Janzen, D.G. VanDerveer, L.F. Mehne and G.J. Grant, "Ruthenium(II) thiocrown complexes: Synthetic, spectroscopic, electrochemical, DFT, and single crystal X-ray structural studies of $[Ru([15]aneS_3)Cl](PF_6)$ ", *Inorg. Chim. Acta* Vol. 364, Issue 1, 55-60, 2010.
- [24] N. Shan, S.M.Hawxwell, H. Adams, L. Brammer and J.A. Thomas, "Self-Assembly of ElectroactiveThiocrownRuthenium(II) Complexes into Hydrogen-Bonded Chain and Tape Networks" *Inorg. Chem.*, Vol. 47, pp. 11551-11560, 2008.
- [25] H.J. Holdt, H. Müller, M. Pötter, A. Kelling, U. Schilde, I. Starke, M. Heydenreich and E. Kleinpeter, "The First Sandwich Complex with an Octa(thioether) Coordination Sphere: Bis(maleonitrile-tetrathia-12-crown-4)silver(I)", *Eur. J. Inorg. Chem.* Issue 12, pp. 2377-2384, 2006.
- [26] H. Müller, A. Kelling, U. Schilde and H.J. Holdt, "Ag(I)-, Hg(II)- und Pt(II)-Komplexe von Maleonitrilthiakronethern", *Z. Naturforsch.*, Vol. 64b, pp- 1003-1015 (2009).
- [27] C.D. Beard, L. Carr, M.F. Davis, J. Evans, W. Levason, L. D. Norman, G. Reid and M. Webster, "Studies on Chromium(III) and Vanadium(III) Complexes with Crown Ether and Crown Thioether Coordination – Synthesis, Properties and Structural Systematics", *Eur. J. Inorg. Chem.*, Issue 21, pp. 4399-4406, 2006.
- [28] C.P. Kulatilleke, "Characterization and properties of the copper(II/I) complexes of macrocyclic hexathiaether ligand [21]aneS₆", *Polyhedron*, Vol. 26, pp. 1166-1172, 2007.
- [29] H. -J. Küppers, K. Wieghardt, Y.-H. Tsay, C. Krüger, B. Nuber and J. Weiss, "Crown Thioether Complexes of Ag^I and Cu^I: The Crystal Structures of $\{[Ag_3L_3]AgL[AgL_2]\}(ClO_4)_4$ and $[LCuI]$ (L = 1, 4, 7-Trithiacyclononane)", *Angew. Chem. Int. Ed. Engl.*, Vol. 26, pp. 575-576, 1987.
- [30] A. J. Blake, J. A. Greig, A. J. Holder, T. I. Hyde, A. Taylor and M. Schroder, "Bis(1,4,7-trithiacyclononane)gold Dication: A Paramagnetic, Mononuclear Au^{II} Complex", *Angew. Chem., Int. Ed. Engl.*, Vol. 29, PP. 197-198, 1990.
- [31] (a) A. J. Blake, R. O. Gould, J. A. Greig, A. J. Holder, T. I. Hyde and M. J. Schroder, "Gold thioether chemistry: synthesis, structure, and redox interconversion of $[Au([9]aneS_3)_2]^{+2/+3+}$ ([9]aneS₃= 1,4,7-trithiacyclononane)", *Chem. Soc. Chem. Commun.*, Issue 13, pp. 876-878, 1989. (b) A. J. Blake, A. Taylor and M. J. Schroder, "Interconversion of au^{I/II/III} centres in thioether macrocyclic complexes: the synthesis, structures and redox properties of $[Au([18]aneS_6)]PF_6$ and $[Au_2([15]aneS_5)_2][B(C_6F_5)_4]_2$ ", *Chem. Soc. Chem. Commun.*, Issue 13, pp. 1097-1098, 1993.
- [32] J.L. Shaw, J. Wolowska, D. Collison, J.A.K. Howard, E.J.L. McInnes, J. McMaster, A.J. Blake, C. Wilson, M. Schröder, "Redox Non-innocence of Thioether Macrocycles: Elucidation of the Electronic Structures of Mononuclear Complexes of Gold(II) and Silver(II)", *J. Am. Chem. Soc.*, Vol. 128, pp. 13827-13839, 2006.